Ultrafast laser inscription of bistable and reversible waveguides in strontium barium niobate crystals

Cite as: Appl. Phys. Lett. **96**, 191104 (2010); https://doi.org/10.1063/1.3429584
Submitted: 25 December 2009 . Accepted: 18 April 2010 . Published Online: 11 May 2010

D. Jaque, N. D. Psaila, R. R. Thomson, F. Chen, L. M. Maestro, A. Ródenas, D. T. Reid, and A. K. Kar

Ultrafast laser inscription of bistable and reversible waveguides in strontium barium niobate crystals

D. Jaque,[1,a)] N. D. Psaila,[2] R. R. Thomson,[2] F. Chen,[3] L. M. Maestro,[1] A. Ródenas,[2] D. T. Reid,[2] and A. K. Kar[2]
[1]*Departamento de Física de Materiales, Universidad Autónoma de Madrid, 28049 Madrid, Spain*
[2]*School of Engineering and Physical Sciences, Heriot-Watt University, Edinburgh EH14 4AS, United Kingdom*
[3]*School of Physics, Shandong University, Jinan 250100, People's Republic of China*

(Received 25 December 2009; accepted 18 April 2010; published online 11 May 2010)

We report the fabrication of buried optical channel waveguides in strontium barium niobate nonlinear ferroelectric crystals by direct ultrafast laser inscription. These waveguides are strongly polarized and can be reversibly switched on and off by changing the temperature of the crystal, a characteristic we attribute to the bistable enhancement of the electro-optic coefficients at the ferro to paraelectric phase transition. © *2010 American Institute of Physics*. [doi:10.1063/1.3429584]

Ultrafast laser inscription (ULI) is a versatile, fast, clean, and almost universal technique for the inscription of optical waveguides in transparent media, including nonlinear crystals and laser gain media.[1–3] ULI relies on the microstructural changes which can be induced when ultrashort laser pulses are tightly focused inside a transparent medium. These changes may manifest themselves through a refractive index modification which can be used to directly inscribe optical waveguides. The nature, magnitude and origin of the refractive index modification depends on the inscription parameters (pulse energy, pulse duration, laser polarization, laser wavelength, scan speed, pulse repetition rate and focusing geometry) as well as on the particular optical response of the irradiated material. The mechanisms at the basis of the refractive index modifications have attracted significant attention over recent years, concluding that refractive index modification arise as the result of a complex combination of different phenomena such as lattice damage, stress-induced lattice distortions, compositional changes, and photochemical reactions.[4–6]

Interestingly, it has previously been proposed that in ferroelectric crystals the refractive index can also be modified through the appearance of space charge fields in combination with the electro-optic effect. Nevertheless, this mechanism has not yet been applied for the fabrication of optical buried waveguides. This would be especially relevant in the ferroelectric strontium barium niobate (SBN) crystal because of its prime importance in modern photonics (due to its nonlinear, electro-optic, photorefractive, laser, and bistable properties).[7–10] This paper reports on the optical properties of ULI buried channel waveguides in SBN. The results reveal a bistable and reversible optical behavior when the system is thermally driven from the ferroelectric to the paraelectric phase which can be explained in terms of the changes in the electro-optic coefficients which take place during the ferroelectric phase transition (PhT).

The SBN ($Sr_{0.60}Ba_{0.40}Nb_2O_6$) sample used in this work is nominally pure and its PhT temperature was measured to be 75 °C. The SBN sample was multidomain, with the domain orientation flipping 180° from the $+c$ to $-c$ directions along the sample. Waveguides were inscribed by using an Yb:fiber laser (Fianium Ltd.) providing ≈350 fs pulses at 1064 nm, with a pulse repetition rate of 500 kHz. For all experiments, the laser polarization was adjusted to be perpendicular to both the incident beam and sample translation direction. The inscription beam was focused ≈300 μm below sample surface by using a 0.4 numerical aperture lens. Structures were inscribed by translating the 6 mm long sample perpendicular to the optical c-axis and at a constant velocity of 6 mm s^{-1}. The pulse energy was varied between 425 and 725 nJ, resulting in all cases in observable refractive index modifications. Preliminary investigations indicated that the waveguides fabricated using 648 nJ pulses exhibited the most interesting guiding properties, and hereafter, we will refer to these as the optimum waveguides. For the remainder of this paper we analyze in detail the properties of the optimum waveguides.

Figure 1(a) shows the optical transmission image of the end facet of the waveguide. Two modified regions can be differentiated. First, at the focal volume a very elongated and narrow modified region ≈3 μm in width and ≈40 μm in length has been created parallel to the pulse propagation direction. Second, an ellipsoidal modified region appears centered around the focal volume with a maximum width of ≈25 μm and an approximate length of 40 μm. The nature of these two regions has been investigated by micro-Raman and scanning electron microscope experiments (not shown here for the sake of brevity). Measurements suggest that the central region corresponds to a slightly damaged region

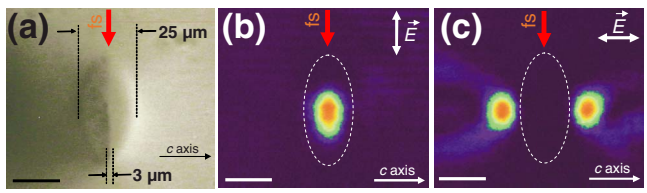

FIG. 1. (Color online) (a) Optical transmission image of the laser induced modified track generated with a pulse energy of 648 nJ. The spatial extent of the damage region and of the heat affected zone are indicated. Near field spatial distribution of 980 nm waveguide modes obtained for (b) ordinary and (c) extraordinary polarizations, with the heat affected zone shown, for comparison, by the dashed ellipse.

a)Electronic mail: daniel.jaque@uam.es.

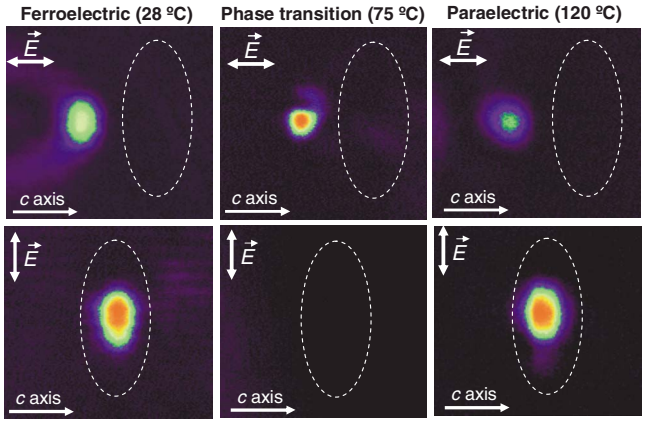

FIG. 2. (Color online) Near-field spatial distribution of the 980 nm waveguide modes obtained for extraordinary (top) and ordinary (bottom) polarizations at three different temperatures corresponding to the ferroelectric phase, to the ferro-to-para PhT and to the paraelectric phase. The extent of the heat affected zone is shown schematically by the dashed ellipse.

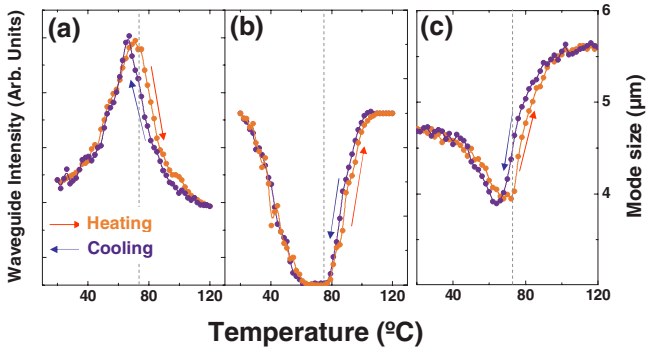

FIG. 3. (Color online) Temperature dependence of the (a) extraordinary and (b) ordinary waveguide mode intensity. The temperature dependence of the average mode size of the extraordinary mode is shown in (c). In each case, the red and blue data correspond to heating and cooling procedures. The dashed line indicates the PhT temperature.

(where the Raman signal slightly decreases), and the ellipsoidal modified region to a strain affected volume characterized by a local compression (slight increase in the Raman phonon modes energy). We attribute these two regions to the presence of a direct laser-damaged area localized at the focal volume, and to the creation of a strained area due to the presence of a heat-affected zone (HAZ) (Ref. 11) which is expected due to the high pulse repetition rates used in this work.[12] The guiding properties of the structures were probed by end-coupling light from a 980 nm fiber-coupled diode into one end of the waveguide. Figures 1(b) and 1(c) present the waveguide's modes at 980 nm for ordinary (o)-polarized and extraordinary (e)-polarized light, respectively. As can be seen in Figs. 1(b) and 1(c), the o-polarized light is guided inside the HAZ, whereas the e-polarized light is guided on either side of the HAZ. By analyzing the intensity profile of scattered light, the propagation losses of the waveguides were measured to be 1.8 and 1.0 dB/cm for o- and e-polarized light, respectively.

The guiding properties of the o- and e-polarizations were also observed to differ in their thermal response. Figure 2 presents the guided modes for e-(top) and o-(bottom) polarizations at three different temperatures corresponding to the ferroelectric phase, the PhT and the paraelectric phase. In this figure the dashed line indicates the spatial extension of the HAZ. For the e-polarization, guiding was found to be enhanced at PhT (more intense and confined mode) and strongly deteriorated in the paraelectric phase, in which only very weak guiding was observed. Surprisingly, for the o-polarization the opposite behavior was found: waveguiding was completely absent at the PhT, only re-emerging when the sample was heated further into its paraelectric phase.

These changes in the waveguiding properties have been found to be completely reversible. This is illustrated in Fig. 3, in which we have included the e- and o-polarized mode intensities, as well as the e-polarization mode size obtained during a heating and cooling cycle [Figs. 3(a)–3(c), respectively]. It should also be noted that the heating and cooling procedures have been found to be nonequivalent, leading to an optical bistable response in the region of the PhT. This behavior can be explained in terms of the characteristic thermal hysteresis associated with the first-order ferroelectric transition of SBN.[7]

The bistable and reversible optical behavior observed for SBN waveguides can be understood in terms of the creation of a space-charge distribution on either side of the strained HAZ. During irradiation, a highly ionized region is generated in the focal region. After irradiation electrons may be displaced along the c-axis due to photovoltaic effect as it is known to occur in $LiNbO_3$ crystals,[13–15] being this charge displacement relevant in the HAZ due to the thermal-induced enhancement of electron mobility. The resultant space-charge distribution, can be thought of as an electric dipole pointing parallel to the c-axis.[15] We suggest that this space-charge field would modify both the o- and e-polarization indices via the electro-optic effect, leading to an induced refractive index change given by the following:

$$\Delta n_{o(e)}^{sc} = -\tfrac{1}{2} n_{o(e)}^3 r_{13(33)} E_{sc}, \tag{1}$$

where $n_{o(e)}$ is the $o(e)$ refractive index, $r_{13(33)}$ is the corresponding electro-optic coefficient, and E_{sc} is the space charge field along the c-axis. Importantly, the complete ordinary refractive index map will also have an additional elasto-optic contribution arising from the local lattice strain induced in the HAZ (Δn_o^{strain}). According to this model, the extraordinary refractive index change at both sides of HAZ would be proportional to the electro-optic coefficient value. In the particular case of SBN, these coefficients are known to be enhanced drastically at PhT, suffering then a strong reduction in the paraelectric phase.[9] This behavior well explains the observed improvement in the waveguiding at PhT and the deterioration of waveguiding in the paraelectric phase (see Figs. 2 and 3). According to this assumption, the spatial modulation of the ordinary refractive index would be determined by the interplay between the strain-induced refractive index increment (Δn_o^{strain}) and the electro-optic index reduction induced in the HAZ (Δn_o^{sc}). Experimental data suggest that at PhT the enhancement in the r_{13} coefficient reduces the overall ordinary refractive index increment in the HAZ, therefore, suppressing waveguiding.

There are also two additional experimental evidences that support this explanation. First, when ULI was performed in absence of thermal accumulation (by using 1 kHz lasers) no waveguides of any kind were formed. Thus, in the absence of any thermal induced enhancement of the electron's

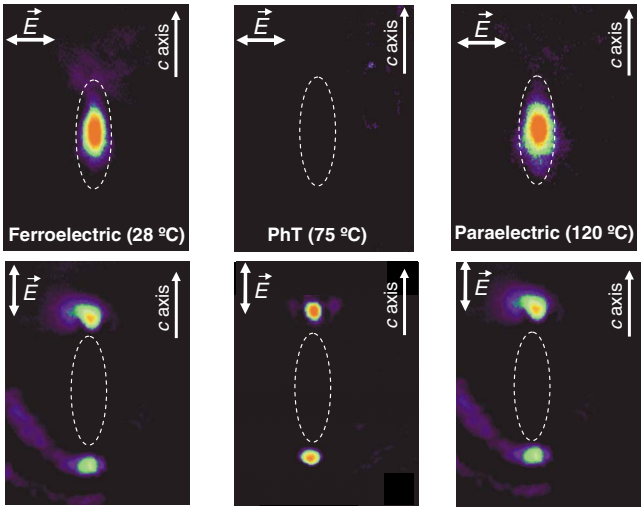

FIG. 4. (Color online) Near field spatial distribution of the 980 nm waveguide modes obtained for extraordinary (top) and ordinary (bottom) polarizations at three different temperatures corresponding to the ferroelectric phase, to the ferro-to-para PhT and to the paraelectric phase. The extension of the heat affected zone is schematically shown. In this case fematosecond pulses were incident parallel to the *c*-axis.

mobility, no space charge fields are created. Second, when the ULI was further performed with the sample *c*-axis parallel to the propagation direction of the inscription pulses, confinement of *e*-polarized light was found to occur at the top and at the bottom of the HAZ instead of at its sides (see Fig. 4), this revealing the presence of a dipolelike space-charge field with the dipole axis parallel to the *c*-axis, i.e., parallel to the photovoltaic field. Independently of the exact orientation of the space-charge field, we have found that the same bistable and reversible behavior described for the waveguides fabricated in the orthogonal geometry (see Figs. 2 and 3). Thus, the charge displacement and accumulation along the *c*-axis provides a satisfactory qualitative explanation for the bistable optical behavior of the waveguides illustrated in Fig. 1. Nevertheless, the exact mechanisms leading to charge pinning at the sides of the HAZ are still not well understood and further experiments are required such as ULI at different temperatures, the study of the influence of different impurities that would modify the photorefractive response of SBN, and the application of external fields.

In summary, we have demonstrated the formation of channel waveguides in SBN crystals by ULI of single line structures. The refractive index modifications responsible for the waveguiding are attributed to the appearance of a heat affect zone and a space-charge induced electric field. A bistable and reversible optical behavior has been found when the SBN system is thermally driven through its ferroelectric PhT which can be explained by the strong enhancement of the electro-optic during PhT. Due to the inherent three-dimensional (3D) capability of the ULI technique, and the ferroelectric nonlinear properties of SBN crystals, the waveguides reported here open an interesting direction for the fabrication of 3D integrated photonic devices exhibiting useful bistable and nonlinear properties.

The authors gratefully acknowledge support from the Scottish Universities Physics Alliance (DJ), by the UK Engineering and Physical Sciences Research Council (project Grant Nos. EP/E016863/1, EP/D047269/1, and EP/G030227/1), by the Spanish Ministerio de Ciencia y Tecnología (Grant No. MAT2007-64686), and by the Universidad Autónoma de Madrid and Comunidad Autónoma de Madrid (Grant No. CCG08-UAM/MAT-4434) and by the National Natural Science Foundation of China (Grant No. 10925524). We also acknowledge support from Fianium Ltd.

[1] S. Nolte, M. Will, J. Burghoff, and A. Tuennermann, Appl. Phys. A: Mater. Sci. Process. **77**, 109 (2003).
[2] R. Osellame, G. Della Valle, N. Chiodo, S. Taccheo, P. Laporta, O. Svelto, and G. Cerullo, Appl. Phys. A: Mater. Sci. Process. **93**, 17 (2008).
[3] B. McMillen, K. P. Chen, H. An, S. Fleming, V. Hartwell, and D. Snoke, Appl. Phys. Lett. **93**, 111106 (2008).
[4] J. Burghoff, C. Grebing, S. Nolte, and A. Tünnermann, Appl. Phys. Lett. **89**, 081108 (2006).
[5] A. Ródenas, G. A. Torchia, G. Lifante, E. Cantelar, J. Lamela, F. Jaque, L. Roso, and D. Jaque, Appl. Phys. B: Lasers Opt. **95**, 85 (2009).
[6] F. Vega, J. Armengol, V. Diez-Blanco, J. Siegel, J. Solis, B. Barcones, A. Perez-Rodriguez, and P. Loza-Alvarez, Appl. Phys. Lett. **87**, 021109 (2005).
[7] N. V. Bogodaev, T. R. Volk, L. I. Ivleva, P. A. Lykov, N. M. Polozkov, and V. V. Osiko, Laser Phys. **11**, 511 (2001).
[8] J. J. Romero, D. Jaque, J. Garcia Sole, and A. A. Kaminskii, Appl. Phys. Lett. **78**, 1961 (2001).
[9] M. Goulkov, T. Granzow, U. Dörfler, T. Woike M. Imlau, R. Pankrath, and W. Kleemann, Opt. Commun. **218**, 173 (2003).
[10] M. O. Ramirez, D. Jaque, L. E. Bausa, and J. García Solé, Phys. Rev. Lett. **95**, 267401 (2005).
[11] A. H. Nejadmalayeri and P. R. Herman, Opt. Express **15**, 10842 (2007).
[12] M. Beresna, T. Gertus, R. Tomasiunas, H. Misawa, and S. Juodkazis, Laser Chem. **2008**, 976205 (2008).
[13] O. Beyer, I. Breunig, F. Kalkum, and K. Buse, Appl. Phys. Lett. **88**, 051120 (2006).
[14] S. Juodkazis, M. Sudzius, V. Mizeikis, H. Misawa, E. G. Gamaly, Y. Liu, O. A. Louchev, and K. Kitamura, Appl. Phys. Lett. **89**, 062903 (2006).
[15] Q. W. Song, C.-P. Zhang, and P. J. Talbot, Appl. Opt. **32**, 7266 (1993).